

Anomalous heat capacity and x-ray photoelectron spectroscopy of superconducting $\text{FeSe}_{1/2}\text{Te}_{1/2}$

V. P. S. Awana,^{1,a)} Govind,¹ Anand Pal,¹ Bhasker Gahtori,² S. D. Kaushik,² A. Vajpayee,¹ Jagdish Kumar,¹ and H. Kishan¹

¹Quantum Phenomenon and Applications Division, National Physical Laboratory (CSIR),

Dr. K. S. Krishnan Marg, New Delhi 110012, India

²UGC-DAE Consortium for Scientific Research, Mumbai Centre, BARC, Trombay, Mumbai—400085, India

(Presented 16 November 2010; received 14 September 2010; accepted 15 November 2010; published online 28 March 2011)

The bulk polycrystalline sample $\text{FeSe}_{1/2}\text{Te}_{1/2}$ is synthesized via the solid state reaction route in an evacuated, sealed quartz tube at 750°C. The presence of superconductivity is confirmed through magnetization/thermoelectric/resistivity studies. It is found that the superconducting transition temperature (T_c) is around 12 K. The heat capacity (C_p) of superconducting $\text{FeSe}_{1-x}\text{Te}_x$ exhibits a hump near T_c , instead of a well-defined lambda transition. X-ray photoelectron spectroscopy studies reveal well-defined positions for divalent Fe, Se, and Te, but with sufficient hybridization of the Fe ($2p$) and Se/Te ($3d$) core levels. In particular, divalent Fe is shifted to a higher binding energy, and Se and Te to a lower one. The situation is similar to that observed previously for the famous Cu-based high T_c superconductors, where the Cu ($3d$) orbital hybridizes with O ($2p$). We also found the satellite peak of Fe at 712.00 eV, which is attributed to the charge-carrier localization induced by Fe at the $2c$ site. © 2011 American Institute of Physics. [doi:10.1063/1.3556682]

I. INTRODUCTION

Since the discovery of superconductivity in $\text{LaFeAsO}_{1-x}\text{F}_x$ (“1111”),¹ an important development has been the invention of superconductivity in another class of materials, $\text{Fe}(\text{Se}, \text{Te})$ (“11”).² Superconductivity has been observed in the FeSe_{1-x} system at ~ 8 K in its tetragonal form in the absence of doping.² Superconductivity in the FeSe_{1-x} system is significantly affected by applied pressure and chalcogenide substitutions.^{2–6} In particular, an applied pressure of only up to 4.15 GPa enhances the system’s transition temperature (T_c) to ~ 37 K, with a dT_c/dP of around 9 K/GPa.⁶ The effect of chemical pressure has been studied in “11” systems by means of Se-site substitution.⁴ It has been found that the superconducting transition temperature increases with Te doping in the $\text{FeSe}_{1-x}\text{Te}_x$ system, reaches a maximum at about 50% substitution, and then decreases with more Te doping.⁴ Interestingly, FeTe is no longer superconducting. Here we report the synthesis, structure, magnetization, heat capacity, and x-ray photoelectron spectroscopy (XPS) studies of the $\text{FeSe}_{1/2}\text{Te}_{1/2}$ compound, which is the “11” compound with the highest possible T_c value of ~ 14.5 K.

II. EXPERIMENT

The polycrystalline sample of $\text{FeSe}_{1/2}\text{Te}_{1/2}$ was synthesized via the solid state reaction route. The stoichiometric ratio of highly pure ($> 3N$) Fe, Se, and Te was ground, pelletized, and then encapsulated in an evacuated (10^{-3} Torr) quartz tube. The encapsulated tube was heated at

750°C for 12 h and then slowly cooled to room temperature. The initially sintered powder was again ground, pelletized in a rectangular shape, sealed in an evacuated quartz tube, and resintered at 750°C for 12 h. The x-ray diffraction patterns of the samples were obtained with the help of a Rigaku diffractometer using CuK_α radiation. The resistivity measurements were recorded for temperatures down to 4.2 K via the four-probe method. The temperature dependence of the AC magnetization of the $\text{FeSe}_{1/2}\text{Te}_{1/2}$ sample was measured on a physical property measurement system (PPMS). The heat capacity $C_p(T)$ in zero field was also measured using a PPMS. The $\text{FeSe}_{1/2}\text{Te}_{1/2}$ was characterized by XPS (Perkin Elmer-PHI model 1257), working at a base pressure of 5×10^{-10} Torr. The chamber was equipped with dual anode Mg K_α (1253.6 eV) and Al K_α (1486.6 eV) x-ray sources and a high-resolution hemispherical electron energy analyzer. We used a Mg K_α x-ray source for our analysis. The calibration of the binding energy scale was done with the C ($1s$) line at 284.6 eV. The core level spectra of Fe, Te, and Se have been deconvoluted into the Gaussian components.

III. RESULTS AND DISCUSSION

Figure 1 depicts the observed and fitted x-ray diffraction patterns of $\text{FeSe}_{1/2}\text{Te}_{1/2}$ that correspond to the $P4/nmm$ space group. The Rietveld refinement was performed using the FULLPROF SUITE program, and the structure was fitted in the $P4/nmm$ space group with the lattice parameters $a = 3.7926(3)$ Å and $c = 6.015(2)$ Å. These values are in agreement with earlier reports.^{7,8} The refinement was done by taking Fe ions from two different sites ($2a$ and $2c$). The percentage of Fe located at the interstitial $2c$ site was found to be about 8% (Ref. 9). The insets of Fig. 1 show the resistivity (ρ) and AC susceptibility (χ)

^{a)} Author to whom correspondence should be addressed. Electronic mail: awana@mail.nplindia.ernet.in. Fax: 0091-11-45609310. URL: www.freewebs.com/vpsawana/

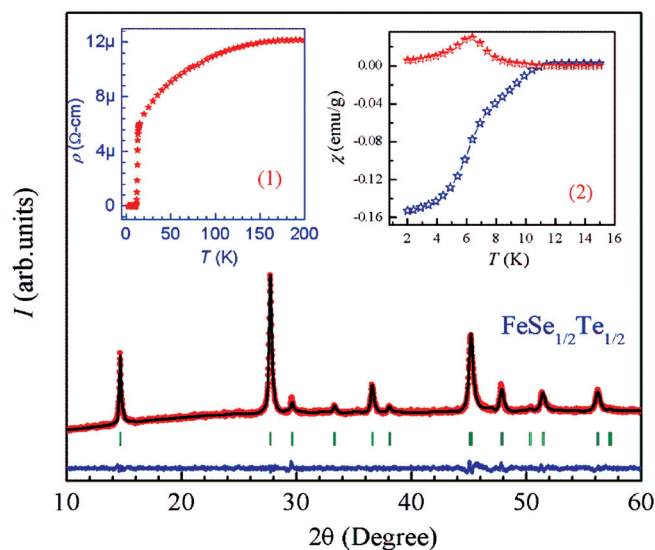


FIG. 1. (Color online) Rietveld fitted room temperature XRD pattern of $\text{FeSe}_{1/2}\text{Te}_{1/2}$. The lefthand inset shows the temperature dependence of the electrical resistivity, and the righthand inset shows susceptibility vs temperature of the same sample.

versus temperature (T) plots for the studied $\text{FeSe}_{1/2}\text{Te}_{1/2}$ compound. Both $\rho(T)$ and $\chi(T)$ demonstrate that the compound is bulk superconducting below 12 K. A detailed physical property characterization of the studied $\text{FeSe}_{1/2}\text{Te}_{1/2}$ compound was reported previously.¹⁰

Figure 2 shows the heat capacity (C_p) versus temperature (T) plot for $\text{FeSe}_{1/2}\text{Te}_{1/2}$. The room temperature (300 K) C_p is around 55 J/mol-K, which is in general agreement with reported values for this compound.⁹ The

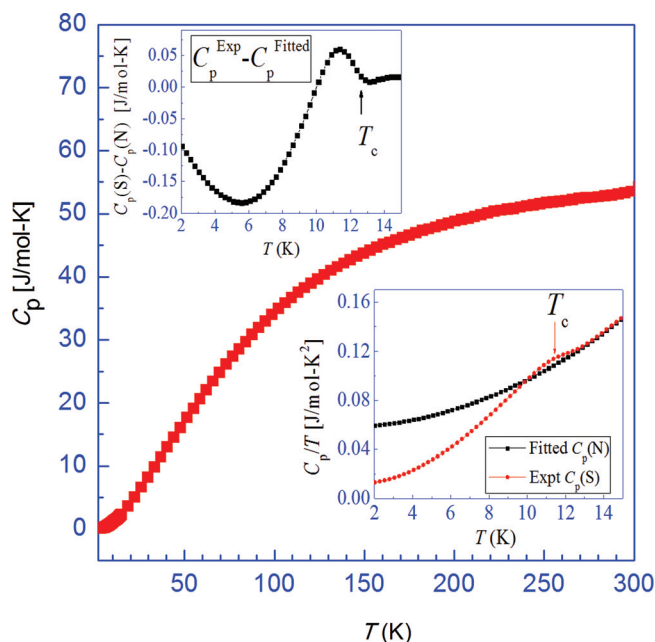


FIG. 2. (Color online) Heat capacity behavior with temperature for $\text{FeSe}_{1/2}\text{Te}_{1/2}$. The upper inset gives the entropy contribution due to the superconducting condensate, and the lower inset shows the observed C_p data along with fitted normal state behavior up to 2 K.

data were fitted to the equation $C_p = \gamma T + BT^3 + CT^5$ from the above superconducting transition from 13 K to 16 K; γT and $(BT^3 + CT^5)$ are the electronic and phononic specific heat contributions, respectively. The value of γ was found to be 57.73 mJ/mol-K², which is somewhat higher than other reported values.^{11,12} However, the value we found for the Debye temperature (171 K) is in agreement with reported values.¹¹ From this fitting, we estimated the corresponding normal state behavior below T_c . The lower inset in Fig. 2 shows the measured value of C_p/T versus T and the corresponding normal state fitted value extrapolated up to 2 K. As far as the entropy contribution due to the superconducting condensate is concerned, the superconducting state minus the normal state is plotted in the upper inset of Fig. 2. At the superconducting transition temperature (T_c), the discontinuity in the electronic C_p versus T plot is seen and marked. The shape of the Lambda transition for studied $\text{FeSe}_{1/2}\text{Te}_{1/2}$ does not exhibit sharp discontinuity at T_c , as has been seen for other superconductors;^{13,14} instead, it presents as a broad, humplike structure.¹³

X-ray photoelectron spectroscopy studies revealed well-defined positions for Fe, Se, and Te, but with sufficient hybridization. Figures 3(a)–3(c) show the deconvoluted core level XPS spectra of Fe ($2p$), Te ($3d$), and Se ($3d$), respectively, for the $\text{FeSe}_{1/2}\text{Te}_{1/2}$ sample. The Fe ($2p_{3/2}$) spectra [Fig. 3(a)] could be resolved into three spin-orbit components at 706.65 eV, 708.50 eV, and 712.00 eV after the carbon correction. An Fe ($2p_{1/2}$) core level spectrum was also deconvoluted into three peaks in a similar way. The $3d$ core level spectrum of Te is deconvoluted into three peaks with respective binding energies of 572.00 eV, 572.65 eV, and 573.90 eV. The peak at energy 572.65 eV corresponds to pure Te metal, while the peak at the lower binding energy of 572.00 eV may have appeared due to the hybridization. In the case of Se, the core level spectra are deconvoluted into two peaks with respective binding energies (BEs) of 53.52 eV and 55.28 eV. The peak for the higher BE corresponds to pure Se, while the peak at the lower BE appeared due to the hybridization.

In Fig. 3(a), the peak at binding energy 706.65 eV corresponds to pure Fe metal. The peak observed at 708.50 eV corresponds to FeO (Fe^{2+}), whereas the peak at 712.00 eV corresponds to a satellite transition that is a characteristic feature of the Fe XPS spectra.^{15,16} The presence of the pure Fe metal peak is in accordance with earlier studies on LaFeAsO (Ref. 17), CaFe_2As_2 (Ref. 18), and LaFePO (Ref. 19); however, no satellite peak (712.00 eV) was observed in these studies. The absence of the satellite peak (712.00 eV) and the resemblance of the 706.65 eV Fe metal peak are correlated with the itinerant character of Fe $3d$ electrons.¹⁸ However, the presence of the satellite peak with the Fe^{2+} peak in the studied samples and the simultaneous appearance of the Fe metal peak (706.65 eV) may be caused by a charge-carrier localization induced by excess Fe at the $2c$ site.¹² The existence of the itinerant character of the Fe $3d$ electronic state is caused by hybridization of the $3d$ states of Fe ions at the $2a$ site and in the Se/Te $4p/5p$ states.¹⁸

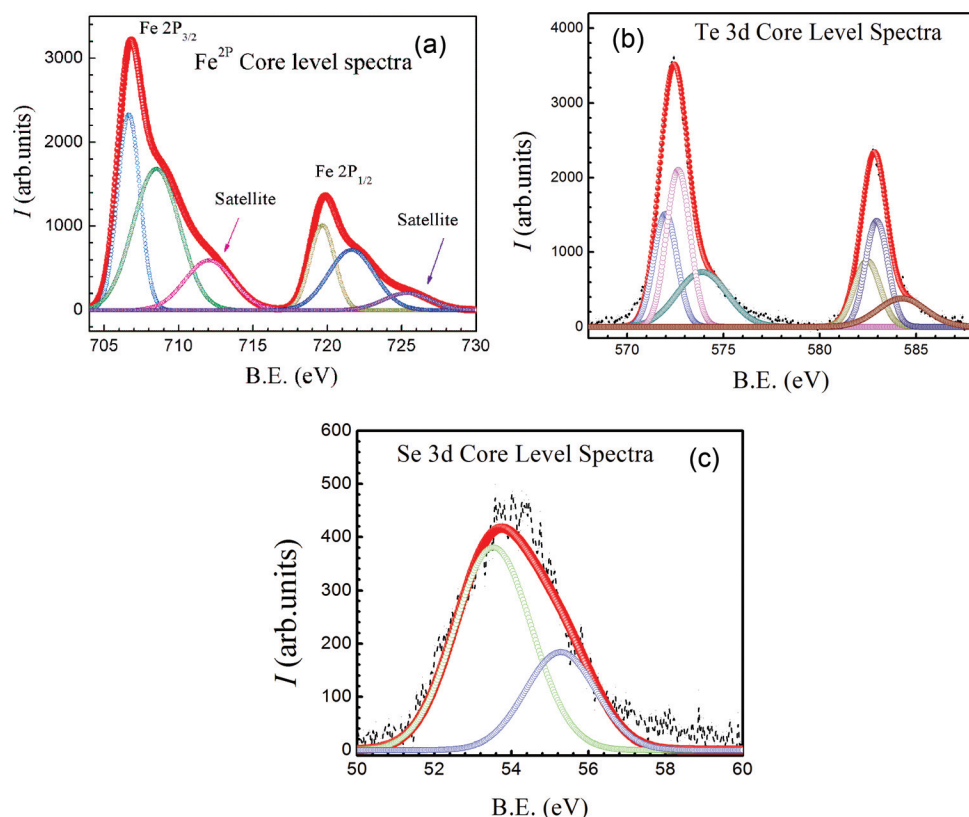


FIG. 3. (Color online) (a) Fe $2p$, (b) Te $3d$, and (c) Se $3d$ XPS spectra for $\text{FeSe}_{1/2}\text{Te}_{1/2}$. The dotted line represents the experimental curve, and the spheres represent the resultant fitted curves. Further, the main fitted plot is deconvoluted in subplots as mentioned in the text.

IV. CONCLUSIONS

In conclusion, we found that in $\text{FeSe}_{1/2}\text{Te}_{1/2}$, about 8% per mole of the Fe present occupies the interstitial $2c$ site. These Fe ions have localized magnetic moments that lead to a broad, cusplike anomaly in the electronic specific heat, rather than a well-defined, sharp lambda transition. This observation is further supported by our XPS measurements, which show that Fe ions have two types of behavior; one arises due to the itinerant nature of Fe $3d$ electrons subsequent to hybridization of the Fe $3d$ and Se/Te $4p/5p$ states, and the other results from charge-carrier localization induced by excess Fe at the $2c$ site.

ACKNOWLEDGMENTS

Anand Pal, A. Vajpayee, and Jagdish Kumar thank the Council of Scientific and Industrial research (CSIR) India for a Senior Research Fellowship. Bhasker Gahtori is supported by the Department of Science and Technology (DST) fast track position (FTP) for young scientists.

¹Y. Kamihara, T. Watanabe, M. Hirano, and H. Hosono, *J. Am. Chem. Soc.* **130**, 3296 (2008).

²F. C. Hsu, J. Y. Luo, K. W. Yeh, T. K. Chen, T. W. Huang, P. M. Wu, Y. C. Lee, Y. L. Huang, Y. Y. Chu, D. C. Yan, and M. K. Wu, *Proc. Natl. Acad. Sci. U.S.A.* **105**, 14262 (2008).

³Y. Mizuguchi, F. Tomioka, S. Tsuda, T. Yamaguchi, and Y. Takano, *Appl. Phys. Lett.* **93**, 152505 (2008).

⁴K. W. Yeh, T. W. Huang, Y. L. Huang, T. K. Chen, F. C. Hsu, P. M. Wu, Y. C. Lee, Y. Y. Chu, C. L. Chen, and J. Y. Luo, *Europhys. Lett.* **84**, 37002 (2008).

⁵Y. Mizuguchi, F. Tomioka, S. Tsuda, T. Yamaguchi, and Y. Takano, *Appl. Phys. Lett.* **94**, 012503 (2009).

⁶S. Masaki, H. Kotegawa, Y. Hara, H. Tou, K. Murata, Y. Mizuguchi, and Y. Takano, *J. Phys. Soc. Jpn.* **78**, 063704 (2009).

⁷M. H. Fang, H. M. Pham, B. Qian, T. J. Liu, E. K. Vehstedt, Y. Liu, L. Spinu, and Z. Q. Mao, *Phys. Rev. B* **78**, 224503 (2008).

⁸T. Ozaki, K. Deguchi, Y. Mizuguchi, H. Kumakura, and Y. Takano, arXiv:1008.1447v2, IEEE Trans. Appl. Supercond. (to be published).

⁹V. Tsurkan, J. Deisenhofer, A. Gunther, Ch. Kant, H. A. Krug von Nidda, F. Schrettleand, and A. Loidl, *Eur. Phys. J. B* **79**, 289 (2010).

¹⁰V. P. S. Awana, A. Pal, A. Vajpayee, M. Mudgel, H. Kishan, M. Husain, R. Zeng, S. Yu, Y. F. Guo, Y. G. Shi, K. Yamaura, and E. Takayama-Muromachi, *J. Appl. Phys.* **107**, 09E128 (2010).

¹¹B. C. Sales, A. S. Sefat, M. A. McGuire, R. Y. Jin, D. Mandrus, and Y. Mozharivskiy, *Phys. Rev. B* **79**, 094521 (2009).

¹²T. J. Liu, X. Ke, B. Qian, J. Hu., D. Fobes, E. K. Vehstedt, H. Pham, J. H. Yang, M. H. Fang, L. Spinu, P. Schiffer, Y. Liu, and Z. Q. Mao, *Phys. Rev. B* **80**, 174509 (2009).

¹³F. Bouquet, Y. Wang, R. A. Fisher, D. G. Hinks, J. D. Jorgensen, A. Junod, and N. E. Phillips, *Europhys. Lett.* **56**(6), 856 (2001).

¹⁴K. Gofryk, A. S. Sefat, E. D. Bauer, M. A. McGuire, B. C. Sales, D. Mandrus, J. D. Thompson, and F. Ronning, *New J. Phys.* **12**, 023006 (2010).

¹⁵T. Fujii, F. M. F. de Groot, G. A. Sawatzky, F. C. Voegt, T. Hibma, and K. Okada, *Phys. Rev. B* **59**, 3195 (1999).

¹⁶S. K. Singh, P. Kumar, M. Husain, H. Kishan, and V. P. S. Awana, *J. Appl. Phys.* **107**, 063905 (2010).

¹⁷W. Malaeb, T. Yoshida, and T. Kataoka, *J. Phys. Soc. Jpn.* **77**, 093714 (2008).

¹⁸E. Z. Kurmaev, J. A. McLeod, A. Buling, N. A. Skorikov, A. Moewes, M. Neumann, M. A. Korotin, Y. A. Izyumov, N. Ni, and P. C. Canfield, *Phys. Rev. B* **80**, 054508 (2009).

¹⁹D. H. Liu, M. Yi, S. K. Mo, A. S. Erickson, A. Analytis, J. H. Chu, D. J. Singh, Z. Hussain, T. H. Geballe, I. R. Fisher, and Z. X. Shen, *Nature* **455**, 81 (2008).